Analyst

PAPER

View Article Online
View Journal | View Issue

Cite this: *Analyst*, 2014, **139**, 5223

Fluorescence turn-on detection of Sn^{2+} in live eukaryotic and prokaryotic cells†

Haichuang Lan,[a] Ying Wen,[a] Yunming Shi,[b] Keyin Liu,[a] Yueyuan Mao[a] and Tao Yi*[a]

Received 4th June 2014
Accepted 21st July 2014

DOI: 10.1039/c4an01014k

www.rsc.org/analyst

Sn^{2+} is usually added to toothpaste to prevent dental plaque and oral disease. However, studies of its physiological role and bacteriostatic mechanism are restricted by the lack of versatile Sn^{2+} detection methods applicable to live cells, including *Streptococcus mutans*. Here we report two Sn^{2+} fluorescent probes containing a rhodamine B derivative as a fluorophore, linked *via* the amide moiety to *N*,*N*-bis-(2-hydroxyethyl)ethylenediamine (**R1**) and *tert*-butyl carbazate group (**R2**), respectively. These probes can selectively chelate Sn^{2+} and show marked fluorescence enhancement due to the ring open reaction of rhodamine induced by Sn^{2+} chelation. The probes have high sensitivity and selectivity for Sn^{2+} in the presence of various relevant metal ions. Particularly, both **R1** and **R2** can target lysosomes, and **R2** can probe Sn concentrations in lysosomes with rather acidic microenvironment. Furthermore, these two probes have low toxicity and can be used as imaging probes for monitoring Sn^{2+} not only in live KB cells (eukaryotic) but also in *Streptococcus mutans* cells (prokaryotic), which is a useful tool to study the physiological function of Sn^{2+} in biological systems.

Introduction

Sn^{2+} has been used in dentistry since the 1950s as a chemical adjunct to prevent dental caries.[1] Sn^{2+} was found to effectively inhibit *Streptococcus mutans*, which leads to tooth decay in human interproximal dental plaque.[2] Recently, there has been increasing interest in the biological roles of Sn^{2+} because Sn is an essential trace mineral for humans and is found in the greatest amount in the adrenal gland, liver, brain, spleen and thyroid gland.[3] There is some evidence that tin is involved in growth factors and cancer prevention of human beings. Deficiency of tin may result in poor growth and hearing loss, but excess tin accumulation can abhorrently affect respiratory and digestive systems.[4,5] However, studies of the physiological role and bacteriostatic mechanism of tin ions are restricted by the lack of versatile Sn^{2+} detection methods applicable to live cells, including *Streptococcus mutans*. It is of great importance to establish a method for the determination of Sn in biological systems.

Some kinds of techniques have been developed for determination of Sn, such as flame atomic absorption spectrometry, potentiometric membrane sensing[6] and UV/visible spectrophotometry.[7] However, these methods are not suitable for *in situ* detection of Sn in biological systems. In our previous work, we developed a fluorescent chemosensor for Sn^{4+}, which was successfully applied in sensing Sn^{4+} in live cells.[8] Recently, Han's group has reported another water soluble fluorescent chemosensor for Sn^{4+}; unfortunately, biological application of the probe was not explored.[9] There is a further need for a probe that minimizes background noise while providing high fluorescence intensity in live cells consistent with the Sn^{2+} found in the cell.

As we know, rhodamine B is widely used as a fluorescent probe for the detection of metal ions[10] and biomolecules,[11] due to the ring opening reaction of rhodamine.[12] However, rhodamine B is very sensitive to the acidic environment; therefore, it would be advantageous to have a probe that works well under the pH conditions in an organelle that play a role in Sn

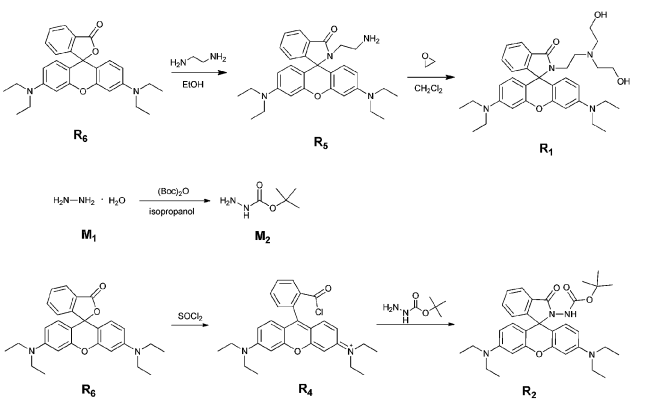

Scheme 1 Synthesis of **R1** and **R2**.

[a]*Department of Chemistry and Concerted Innovation Center of Chemistry for Energy Materials, Fudan University, 220 Handan Road, Shanghai 200433, China. E-mail: yitao@fudan.edu.cn*

[b]*P&G Technology (Beijing) Co., Ltd., No. 35 Yuan Road, B zone, Shunyi District, Beijing, 101312, China*

† Electronic supplementary information (ESI) available: Synthesis details and additional spectra. See DOI: 10.1039/c4an01014k

accumulation in the cell. Herein, two novel rhodamine B-based fluorescent probes (**R1** and **R2** in Scheme 1) for Sn^{2+} were designed and synthesized. Compared to our previously developed probe, the new compounds are easier to synthesize and have improved solubility, better selectivity and sensitivity for Sn^{2+}. Furthermore, **R1** and **R2** possess a flexible chain with acyl and hydroxyl groups, which have higher affinity for Sn^{2+} than for other metal ions. Particularly, **R2** can function in a comparatively lower pH environment that can probe Sn concentrations in lysosomes with a rather acidic microenvironment. Most importantly, **R1** and **R2** can detect Sn^{2+} in both live KB cells and *Streptococcus mutans* by the fluorescent turn-on process. To the best of our knowledge, there is no report of a fluorescent probe for Sn^{2+} imaging in prokaryotic cells, such as *Streptococcus mutans*.

Experimental section

General methods

Unless otherwise stated, materials were obtained from commercial suppliers and were used without further purification. Rhodamine (95%) was obtained from Sinopharm Chemical Reagent Co., Ltd. (Shanghai). Other chemicals were provided by Shanghai No. 1 Chemical Reagent. Flash chromatography was carried out on silica gel (200–300 mesh). The ^{1}H NMR (500 MHz) and ^{13}C NMR (125 MHz) spectra were recorded on a Bruker DRX-500 spectrometer. Proton chemical shifts are reported in parts per million downfield from tetramethylsilane (TMS). HRMS was obtained with an LTQ-Orbitrap mass spectrometer (Thermo Fisher, San Jose, CA). UV/vis spectra were recorded using a Shimadzu UV-2250 spectrophotometer. Fluorescence spectra were recorded using an Edinburgh FLS-920 spectrophotometer. All pH measurements were made with a model Mettler–Toledo meter.

Synthesis of sensors

The synthesis process of **R1** and **R2** is shown in Scheme 1. The procedure for the synthesis of **R5** has been described in the literature.[13] **R1** was prepared by the treatment of **R5** with excess oxirane to give the diol.[14] Hydrazine monohydrate was protected by Boc to afford **M2**.[15] The treatment of **M2** with rhodamine B acid chloride gave fluorescent probe **R2**.[16] The details of the synthesis are shown in ESI.†

Metal ion sensing procedure

The solutions of metal ions (10.0 mM) were prepared in deionized water. Stock solutions of **R1** and **R2** (0.2 mM) were prepared in ethanol and then diluted to 20 μM with ethanol–water (1 : 1, v/v, pH 7.04) for spectral measurements. In titration experiments, each time a 2.0 mL solution of **R1** or **R2** (20 μM) was filled in a quartz optical cell of 1 cm optical path length, and the Sn^{2+} stock solution was added into the quartz optical cell gradually by using a micro-pipette. Spectral data were recorded at 5 min after the addition. For selectivity experiments, the test samples were prepared by adding appropriate volumes of the metal ion stock solution into 2.0 mL solution of **R1** or **R2** (20 μM). For fluorescence measurements, excitation was at 560 nm, and emission was collected from 565 to 700 nm.

pH titration of R1 and R2

Stock solutions of **R1** and **R2** were respectively added to sodium phosphate buffer at various pH to a final concentration of 10 μM. The fluorescence emission spectra were recorded as a function of pH with λ_{ex} at 560 nm. The titration curves were plotted by using fluorescence emission intensities at 580 nm *versus* pH.

Cell culture

The KB cell line was provided by the Institute of Biochemistry and Cell Biology, Shanghai Institutes for Biological Sciences (SIBS), Chinese Academy of Sciences (CAS) (China). Cells were grown in MEM (Modified Eagle's Medium) supplemented with 10% FBS (Fetal Bovine serum) and 5% CO_2 at 37 °C. Cells (5×10^{-8} L^{-1}) were then plated on 18 nm glass coverslips and allowed them to adhere for 24 hours.

Bacterial culture

Streptococcus mutans (ATCC® 700610™) was grown by inoculating a single colony from the BHI agar plate into 5 mL BHI broth and incubating at 37 °C for 48 h.

Fluorescence imaging

Confocal fluorescence imaging was performed with an OLYMPUS IX81 laser scanning microscope and a 60× oil immersion objective lens. The microscope was equipped with multiple visible laser lines (405, 488, and 543 nm). Images were acquired and processed by using the Olympus FV10-ASW software.

Procedure for fluorescence imaging of intracellular Sn^{2+}. (1) 10 μM **R1** or **R2** in the culture media containing 0.2% (v/v) DMSO was added to cells. The cells were incubated at 37 °C for 30 min, and washed with PBS three times to remove the excess probe and bathed in PBS (2 mL) before imaging. (2) After washing with PBS (2 mL × 3) to remove the excess probe, the cells were treated with 50 μM SnF_2 for 30 min. Excitation of **R1** or **R2** loaded cells at 543 nm was carried out with a semiconductor laser, and the emission was collected at 560–660 nm (single channel). (3) 50 μM SnF_2 prepared in the culture media was added to the cells. The cells were incubated at 37 °C for 30 min, and washed with PBS three times to remove the excess SnF_2. After washing with PBS (2 mL × 3) to remove the excess SnF_2, the cells were treated with 10 μM **R1** or **R2** for 30 min, and washed with PBS three times to remove the excess probe and bathed in PBS (2 mL) before imaging. Cell imaging was then carried out as in the former case.

Procedure for lysosome colocalization experiments. (1) 10 μM **R1** or **R2** in the culture media containing 0.2% (v/v) DMSO was added to the cells. The cells were incubated at 37 °C for 30 min, and washed with PBS three times to remove the excess probe and bathed in PBS (2 mL) before imaging. (2) After washing with PBS (2 mL × 3) to remove the excess probe, the

cells were treated with 50 μM SnF_2 at 37 °C for 30 min, and washed with PBS three times to remove the excess SnF_2 and bathed in PBS (2 mL) before imaging. (3) After washing with PBS (2 mL × 3) to remove the excess SnF_2, the cells were treated with 1.0 μM LysoTracker® Green DND at 37 °C for 30 min. The cells were covered with 2 mL of PBS for fluorescence imaging with the appropriate excitation and emission filters for **R1** or **R2** (λ_{ex} = 543 nm, λ_{em} = 560–660 nm), and Lysotracker Green (λ_{ex} = 488 nm, λ_{em} = 500–540 nm). (4) 50 μM SnF_2 in the culture media was added to the cells. The cells were incubated at 37 °C for 30 min, and washed with PBS three times to remove the excess SnF_2. After washing with PBS (2 mL × 3) to remove the excess SnF_2, the cells were treated with 10 μM **R1** or **R2** for 30 min, and washed with PBS three times to remove the excess probe and bathed in PBS (2 mL) before imaging. Cell imaging was then carried out as in the former case. (5) After washing with PBS (2 mL × 3) to remove the excess probes, the cells were treated with 1.0 μM LysoTracker® Green DND at 37 °C for 30 min. Cell imaging was then carried out as in the former case.

Procedure for fluorescence imaging of Sn^{2+} in bacterial cells. Freshly diluted *Streptococcus mutans* (ATCC® 700610™) was sub-cultured in the presence of 10 μM **R1** or **R2** at 37 °C on a shaker bed at 400 rpm for 60 min. Then the bacteria were collected by centrifugation at 8000 rpm for 2 min and rinsed with saline (pH = 7.0), and the process was repeated three times before imaging. After washing with saline (2 mL × 3) to remove the excess probe, the bacteria were cultured in the presence of 50 μM SnF_2 at 37 °C on a shaker bed at 400 rpm for 60 min. Then the bacteria were collected by centrifugation at 8000 rpm for 2 min and rinsed with saline (pH = 7.0), the process was repeated three times before imaging. The light source at 543 nm provided excitation, and emission was collected in the range of 560–660 nm.

Cytotoxicity assay

The *in vitro* cytotoxicity was measured by using the standard methyl thiazolyl tetrazolium[17] (MTT, Sigma-Aldrich) assay in KB cell lines. Cells growing in the log phase were seeded into a 96-well cell-culture plate at 1 × 10^4 per well. The chemosensor **R1** or **R2** (100 μL per well) at various concentrations of 1.0, 2.5, 5.0, 10.0, 25.0, 50.0 and 100.0 μM was added to the wells of the treatment group, and 100 μL per well DMSO diluted with DMEM to a final concentration of 0.2% added to the negative control group. The cells were incubated for 24 and 48 h at 37 °C under 5% CO_2. The MTT/PBS solution mixture was added to each well of the 96-well assay plate, and incubated for an additional 4 h. An enzyme-linked immunosorbent assay (ELISA) reader (Infinite M200, Tecan, Austria) was used to measure the OD at 490 nm (absorbance value) of each well. The following formula was used to calculate the viability of cells.

$$\text{Viability (\%)} = (\text{mean absorbance value of treatment group/mean absorbance value of control}) \times 100$$

Results and discussion

Response to metal ions

The fluorescence 'turn on' probe is conducive for the detection target. The solution of **R1** or **R2** (20 μM) in ethanol–water (1 : 1, v/v, pH 7.04) is colourless and without fluorescence. After addition of Sn^{2+} (0–20 eq.) to the **R1** or **R2** solution, the colour of the solution changed to pink and an orange fluorescence was observed (Fig. 1). The emission titration experiment showed that the emission at 580 nm was turned on and grew drastically after excitation with 560 nm light for both **R1** and **R2** due to the ring open reaction of rhodamine induced by Sn^{2+} chelation[8,9] (Fig. 1a and c). The fluorescence quantum yield (Q_F) increased from 0.076 to 0.237 for **R1** and 0.066 to 0.187 for **R2** by the addition of Sn^{2+}. The corresponding titration absorption spectroscopy was carried out under the same condition. A new absorption peak at 560 nm gradually appeared for **R1** and **R2** after the addition of Sn^{2+} (Fig. 1b and d). At less than 20 eq. of Sn^{2+}, an excellent linear correlation between the emission intensity (580 nm) of **R1** and **R2** and the Sn^{2+} concentration was obtained with R_{R1}^2 = 0.96631 and R_{R2}^2 = 0.99231, which indicated that the fluorescence intensity at 580 nm increased as a linear function of Sn^{2+} concentration in this concentration range (insets of Fig. 1a and c). Although **R1** and **R2** possess the same response model to Sn^{2+}, it is necessary to explore which one is more sensitive to Sn^{2+}. The detection limit of **R1** and **R2** for Sn^{2+} was determined as 5.7 × 10^{-7} M and 4.6 × 10^{-7} M (Fig. S1†), respectively, indicating that both chemosensors **R1** and **R2** were sensitive for the detection of Sn^{2+}. Furthermore, the present two sensors are superior to that of a previous report.[18]

High-level selectivity is of paramount importance for an excellent chemosensor. Both **R1** and **R2** show high selectivity towards sensing Sn^{2+}. The solutions of **R1** and **R2** (20 μM) in

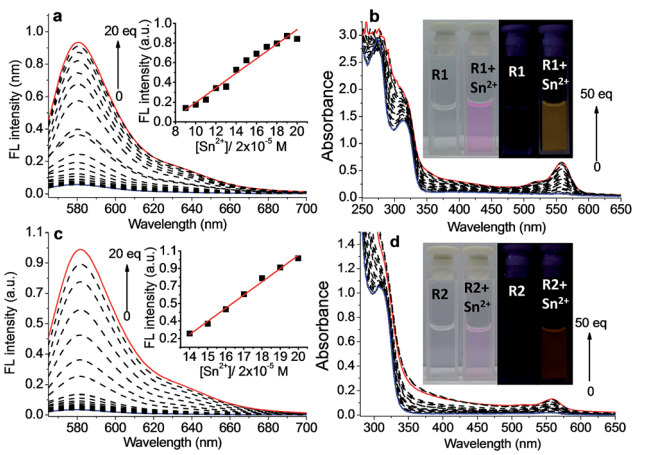

Fig. 1 Fluorescence spectra of (a) **R1** and (c) **R2** (20 μM) upon addition of 0–20 eq. of Sn^{2+}; absorption spectra of (b) **R1** and (d) **R2** upon addition of 0–50 eq. of Sn^{2+}; solvent conditions: ethanol–water (1 : 1, v/v), pH 7.04. Insets of (a) and (c) show the emission intensities at 580 nm as a function of Sn^{2+} concentrations, respectively; insets of (b) and (d) show the colour and fluorescence change of **R1** and **R2** after the addition of Sn^{2+}, respectively.

ethanol–water (1 : 1, v/v, pH 7.04) were turned on just in the presence of Sn^{2+} and Cr^{3+}, while other transition and heavy metal ions, such as K^+, Ag^+, Ca^{2+}, Mg^{2+}, Zn^{2+}, Pb^{2+}, Ni^{2+}, Mn^{2+}, Co^{2+}, Cd^{2+} and Hg^{2+}, displayed minimal enhancement with excitation at 560 nm (Fig. 2). The data showed that the selectivity of **R1** is better than that of **R2**. The photograph of fluorescence changes of **R1** and **R2** (2.0×10^{-5} M) upon addition of various metal ions (10 eq.) are shown in Fig. 2d. Although the detection of Sn^{2+} was interfered with Cr^{3+}, the selectivity has been improved when compared with our previous work.[9]

Besides high sensitivity and selectivity, short response time is another necessity for a fluorescent probe to dynamically image intracellular Sn^{2+} ions or monitor Sn^{2+} in environmental samples in real-time. To study the response time of the probes **R1** and **R2** to Sn^{2+}, the fluorescence enhancement of **R1** and **R2** at 580 nm with resting time after the addition of Sn^{2+} (10 μM) was recorded, and results are shown in Fig. 3. The fluorescence signals increased with the resting time in the beginning and reached a constant level within 3 and 2 min, respectively, for **R1** and **R2** after the addition of Sn^{2+}. This means, the two probes have quick response times towards Sn^{2+} and could be used for real-time tracking of Sn^{2+} in biological samples.

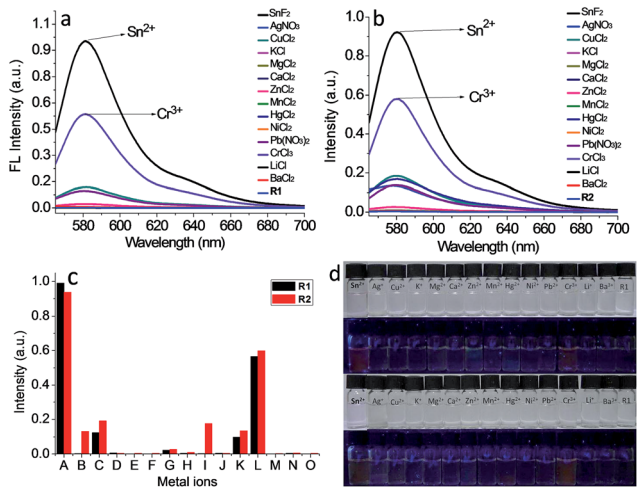

Fig. 2 Fluorescence spectra of (a) **R1** and (b) **R2** after addition of various metal ions in ethanol–water (1 : 1, v/v, pH 7.04) solution ($\lambda_{ex} = 560$ nm); (c) the fluorescent intensity changes of **R1** (black) and **R2** (red) at 580 nm upon addition of various metal ions: (A) Sn^{2+}; (B) Ag^{2+}; (C) Cu^{2+}; (D) K^+; (E) Mg^{2+}; (F) Ca^{2+}; (G) Zn^{2+}; (H) Mn^{2+}; (I) Hg^{2+}; (J) Ni^{2+}; (K) Pb^{2+}; (L) Cr^{3+}; (M) Li^+; (N) Ba^{2+}; (O) blank; (d) photographs of the colour and fluorescence changes of **R1** (above) and **R2** (below) with the addition of various metal ions (10 eq.) in ethanol–water (1 : 1, v/v, pH 7.04).

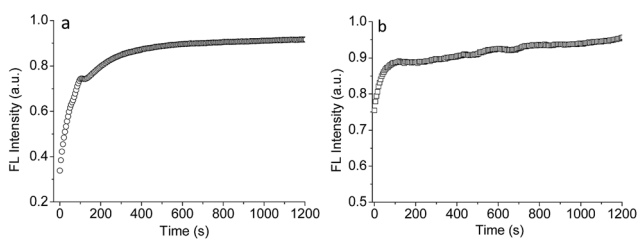

Fig. 3 Kinetics of fluorescence enhancement of (a) **R1** and (b) **R2** (10 μM) at 580 nm in the presence of Sn^{2+} (10 μM) ($\lambda_{ex} = 560$ nm).

Sensing mechanism

In order to understand the binding stoichiometry of R–Sn^{2+} complexes, Job plot experiments were carried out as shown in Fig. 4. The emission intensities at 580 nm were plotted against the molar fraction of **R1** (Fig. 4a) and **R2** (Fig. 4b) with a constant total concentration of [R + Sn^{2+}] (2.0×10^{-5} M). Maximum emission intensities at 580 were reached when the molar fraction was 0.5 for both **R1** and **R2**, indicating the formation of 1 : 1 complexes between the probe and Sn^{2+} (Fig. 4c and d). The equilibrium constants (K) between **R1** (or **R2**) and Sn^{2+} were obtained by using nonlinear curve fitting.[19] On the basis of 1 : 1 stoichiometry, the K value of the complex between **R1** (or **R2**) and Sn^{2+} was estimated to be $K_{\mathbf{R1}} = 4.4 \times 10^4$ ($r^2 = 0.981$) and $K_{\mathbf{R2}} = 3.8 \times 10^4$ ($r^2 = 0.988$) (Fig. S2†). The binding process between **R1** (or **R2**) and Sn^{2+} was further proven by Maldi-Tof-MS spectroscopy of the complex (Fig. S3†). The mass data for **R1** + Sn^{2+} solution showed two peaks at m/z = 729.29 and 727.29; calc. for $C_{34}H_{43}F_2N_4O_4Sn$ [**R1** + SnF_2 − H^+], 729.23, 727.23. The mass data for **R2** + Sn^{2+} showed one peak at m/z = 737.37; calc. for $C_{33}H_{40}N_4O_4SnF_2Na$ [**R2** + SnF_2 + Na^+]: 737.19.

Impact of pH on fluorescence

The spirolactam ring of rhodamine derivatives opens in a certain pH range and indicates the fluorescence of rhodamine.[20] It is therefore necessary to check the fluorescence properties of **R1** and **R2** in solution at different pH values. Furthermore, in a cell, the acidity of different organelles shows great disparity.[21] For example, the normal pH of lysosomes is 4.5–5.5, which may induce the ring opening of **R1** or **R2**.[22] Considering that the application of Sn^{2+} probe **R1** and **R2** intracellularly or extracellularly may be disturbed by the pH, the acid–base titration experiments were carried out by adjusting the pH with an aqueous solution of NaOH and HCl of phosphate-buffered

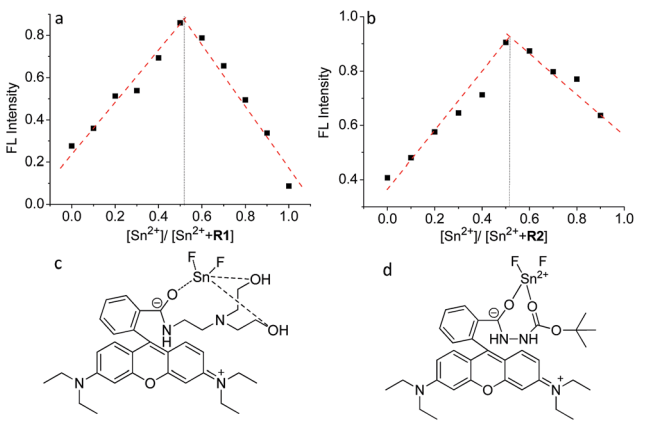

Fig. 4 Job's plots of **R1** (a) and **R2** (b) for the emission intensity change at a wavelength of 580 nm. The total concentration of **R1** (or **R2**) and Sn^{2+} was 20 μM. The proposed structures of complexes of (c) **R1** + Sn^{2+} and (d) **R2** + Sn^{2+} are shown.

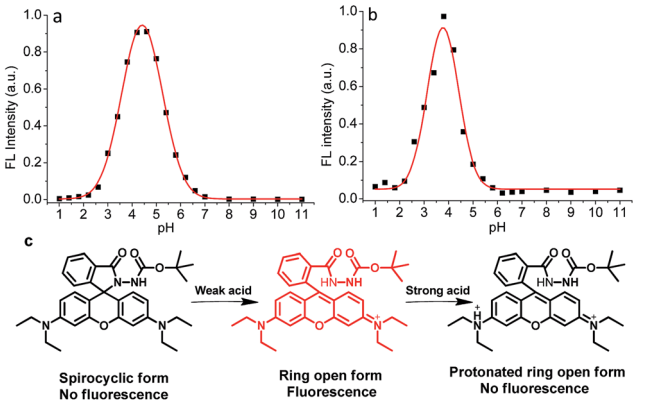

Fig. 5 Dependence of fluorescence at 580 nm of (a) **R1** and (b) **R2** (10 μM) on the pH of PBS solution (λ_{ex} = 560 nm). (c) The proposed mechanism for the fluorescence of **R1** and **R2** affected by pH.

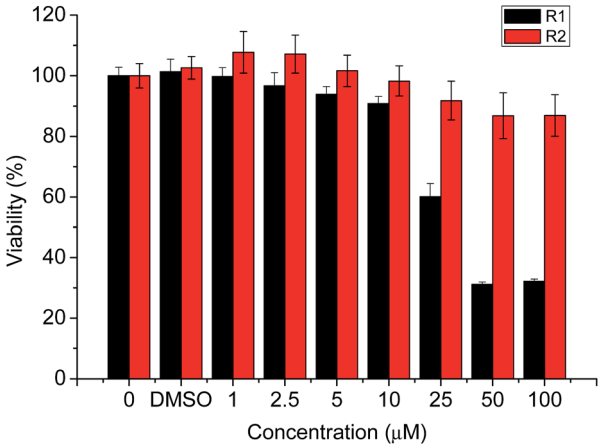

Fig. 6 Cell viability values (%) estimated for KB cells by MTT proliferation test *versus* concentrations (0–100 μM) of **R1** (black) and **R2** (red) after 24 h incubation at 37 °C.

saline (PBS) (Fig. 5a and b). The titration revealed that the pH range for inducing **R1** and **R2** fluorescence turn-on is 2.5–6 and 2–4.5, respectively. It can be predicted that **R1** will be turned on by lysosomes in cells without Sn^{2+} being present, while **R2** can detect Sn^{2+} in a wider pH range.

The proposed mechanism for the fluorescence of **R1** and **R2** affected by pH is explained in Fig. 5c. The mechanism of fluorescence change is based on the change in the structure between spirocyclic and open-cycle forms.[12] The spirocyclic form at high pH is non-fluorescent. With the decrease of pH in the range of 2.5–5.0, the spirocyclic form of both **R1** and **R2** was ring opened by H^+ with the fluorescence switched on due to the enlarged conjugate system (the formation of a push–pull electronic structure). With further decrease of the pH (pH < 2.5), the *N*,*N*-dimethyl group of **R1** and **R2** was protonated, breaking the push–pull electronic structure, resulting in fluorescence off of the probes. Furthermore, due to the weak electron donating effect of the Boc-protected NH group of **R2**, the **R2** probe is more stable than **R1** in the weak acidic environment.

Cytotoxicity of R1 and R2

An ideal cellular chemosensor for practical applications should minimally perturb living systems at the concentration employed. Accordingly, the cytotoxicities of **R1** and **R2** solutions were determined using the MTT assay in KB cells. In the presence of **R2** at a concentration of 1.0–100.0 μM, the cellular viability was estimated to be greater than 90% (Fig. 6) after incubation for 24 h. **R1** also showed low cellular toxicity after 24 h at a concentration of 1.0–10.0 μM. These results indicate that **R2** is less toxic than **R1**, and more suitable for the intracellular detection of Sn^{2+}.

Fluorescence imaging of intracellular Sn^{2+}

Sn^{2+} is usually added to toothpaste as an inhibitory factor,[1] so that oral epithelial cells most likely come into contact with Sn^{2+}. KB cells are the best candidate for the exploration of Sn^{2+} distribution at the cellular level by fluorescence imaging. Here, the practical applicability of **R1** and **R2** as a Sn^{2+} probe in fluorescence imaging of live KB cells was investigated. Firstly, the KB cells were stained with 10 μM **R1** or **R2** at 37 °C for 30 min. As determined by confocal laser scanning microscopy (CLSM), **R1** gave fluorescence emission at a site where KB cells were without Sn^{2+} (Fig. 7a1–g1); whereas, **R2** was scarcely fluorescent (Fig. 7a2–g2). This result confirmed our prediction based on the pH titration experiment in which lysosomes' acidity may have induced **R1** fluorescence emission in the

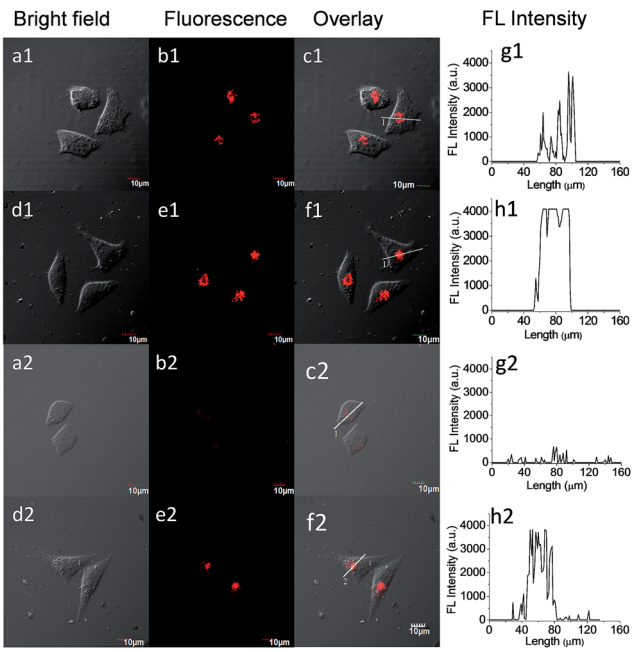

Fig. 7 CLSM images of KB cells. (a1–c1) and (a2–c2) cells separately incubated with 10 μM **R1** and **R2** for 30 min, respectively; (d1–f1) and (d2–f2) show the subsequent incubation with 50 μM SnF_2 for 30 min, respectively. Emission was collected in red channel at 560–660 nm (b1, e1, b2 and e2); a1, d1, a2 and d2 are bright field images and c1, f1, c2 and f2 are overlay images, respectively (λ_{ex} = 543 nm); g1, g2, h1 and h2 are the fluorescent intensity of the line on cells.

absence of Sn^{2+}. When the cells were supplemented with **R1** or **R2** in PBS for 30 min at 37 °C and then incubated with 50 μM Sn^{2+} under the same conditions, **R2** gave a significant fluorescence which increased from a certain intracellular region (Fig. 7d2–h2); **R1** showed a slight change in the fluorescence intensity (Fig. 7d1 and h1). Cell imaging experiments indicate that **R2** is more suitable for the detection of Sn^{2+} at the cellular level, due to its less background noise, particularly in more acidic environments such as in lysosomes. Furthermore, **R1** and **R2** may be specifically targeted to lysosomes, because **R1** and **R2** bear groups similar to 'dimethylethylamino' that is the targeting anchor for lysosomes.[21,22]

Lysosome colocalization experiments

To probe the intracellular locations of **R1** and **R2**, KB cells were co-stained with **R1** or **R2**, Sn^{2+} and LysoTracker® Green DND, which is a commercially available marker for lysosomes and has good separation in excitation and emission spectra with **R1** and **R2**. As shown in Fig. 8a1–d1, the fluorescence images of **R1** and LysoTracker overlapped very well. This result has verified our prediction based on the pH titration experiment and fluorescence imaging of intracellular Sn^{2+}, which showed that **R1** accumulated in lysosomes and the acidity induced **R1** fluorescence emission. Furthermore, Sn^{2+} can also locate in lysosomes and enhance the fluorescence of **R1** and **R2**. More importantly, the fluorescence of **R2** induced by Sn^{2+} and LysoTracker overlapped very well, which indicates that **R2** can detect Sn^{2+} in lysosomes; at the same time, the fluorescence signal of **R2** demonstrated the distribution of Sn^{2+} (Fig. 8a2–d2). Altogether, **R1** and **R2** were verified as lysosome targeting and sensitive to Sn^{2+}. However, it is not yet confirmed that Sn^{2+} is widely distributed in the cell or accumulated only in lysosomes.

To solve the problem mentioned above, a comparative colocalization experiment was carried out. Firstly, the KB cells were stained with 50 μM Sn^{2+} at 37 °C for 30 min, and then incubated with 10 μM **R1** and 1 μM LysoTracker® Green DND or **R2** and 1 μM LysoTracker® Green DND under the same conditions. As determined by CLSM, **R1** and **R2** gave fluorescence emission at a site in KB cells, which overlapped with LysoTracker® Green DND very well (Fig. 9). There was no fluorescence emission at other intracellular sites. This result

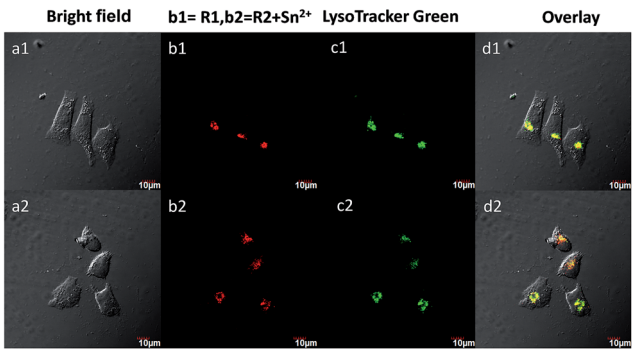

Fig. 8 CLSM images of KB cells. (a1–d1) Cells incubated with 10 μM **R1** and 1 μM LysoTracker Green for 30 min; (a2–d2) successively incubated with 10 μM **R2**, 50 μM SnF_2 and 1 μM LysoTracker Green, each for 20 min. Emission was collected in red channel (b1 and b2) at 560–660 nm (λ_{ex} = 543 nm) or in green channel at 500–540 nm (λ_{ex} = 488 nm); (a1 and a2) are bright field images, and (d1 and d2) are overlay images, respectively.

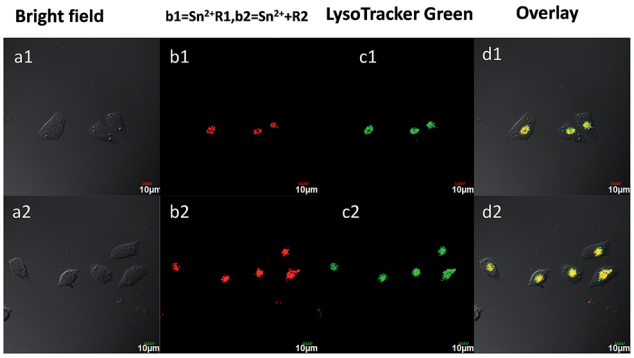

Fig. 9 CLSM images of KB cells. (a1–d1) Cells successively incubated with 50 μM SnF_2, 10 μM **R1** and 1 μM LysoTracker Green, each for 20 min; (a2–d2) successively incubated with 50 μM SnF_2, 10 μM **R2** and 1 μM LysoTracker Green, each for 20 min. Emission was collected in red channel (b1 and b2) at 560–660 nm (λ_{ex} = 543 nm) or in green channel at 500–540 nm (λ_{ex} = 488 nm); a1 and a2 are bright field images and d1 and d2 are overlay images, respectively.

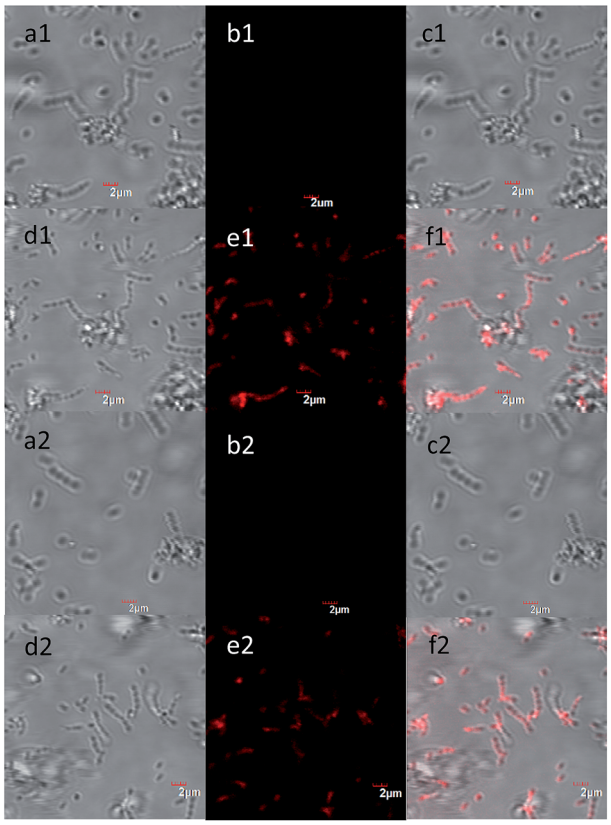

Fig. 10 CLSM images of *Streptococcus mutans* (ATCC® 700610™). (a1–c1) and (a2–c2) cells separately incubated with 10 μM **R1** and **R2** for 30 min, respectively; (d1–f1) and (d2–f2) subsequent incubation with 50 μM SnF_2 for 30 min. Emission was collected in red channel at 560–660 nm (b1, e1, b2 and e2); a1, d1, a2 and d2 are bright field images and c1, f1, c2 and f2 are overlay images, respectively (λ_{ex} = 543 nm).

indicates that Sn^{2+} is internalized into cells, leading to accumulation of the ions in lysosomes. This may be a transmission path of Sn. Many pharmaceutical agents, including various large and small molecules, must be delivered specifically into a particular cellular organelle in order to efficiently exert their therapeutic action. Such delivery is still an unresolved problem, but targeting detection is a helpful attempt.[23]

Fluorescence imaging of Sn^{2+} in bacterial cells

It has been reported that Sn^{2+} can effectively inhibit *Streptococcus mutans*.[1] We have proceeded to investigate the practical applicability of **R1** and **R2** as a Sn^{2+} probe in the fluorescence imaging of live *Streptococcus mutans* (ATCC® 700610™). Firstly, the *Streptococcus mutans* (ATCC® 700610™) cells were stained with 10 μM **R1** or **R2** at 37 °C for 60 min. As determined by CLSM, **R1** and **R2** gave no fluorescence emission without Sn^{2+} present (Fig. 10a1–c1 and a2–c2). When *Streptococcus mutans* cells were supplemented with **R1** or **R2** in PBS for 60 min at 37 °C and then incubated with 50 μM Sn^{2+} under the same conditions, **R1** and **R2** gave a significantly increasing fluorescence (Fig. 10d1–f1 and d2–f2). The overlay of fluorescence and bright field images revealed that the fluorescence signals were localized in the *Streptococcus mutans* (ATCC® 700610™) cells (Fig. 10f1 and f2), indicating that Sn^{2+} exerts its physiological role within the bacterial cell.

Conclusions

In summary, two chemosensors (**R1** and **R2**) for Sn^{2+} were synthesized and characterized. Both of them exhibited high selectivity for Sn^{2+}, while **R2** showed higher sensitivity to Sn^{2+} than **R1**. In addition, **R2** is more suitable for the detection of Sn^{2+} in eukaryotic cells, due to its low cytotoxicity and less background noise, particularly in more acidic environments like that of lysosomes. The application of **R1** and **R2** in prokaryotic cells successfully imaged Sn^{2+} in *Streptococcus mutans* (ATCC® 700610™). Furthermore, **R1** and **R2** as lysosome trackers are able to demonstrate the distribution of Sn^{2+} in eukaryotic cells and in bacteria, which is helpful to research pharmaceutical agent delivery and antibacterial mechanism of Sn^{2+}.

Acknowledgements

The authors are thankful for the financial support from the National Basic Research Program of China (2013CB733700), the China National Funds for Distinguished Young Scientists (21125104), the National Natural Science Foundation of China (51373039), the Program for Innovative Research Team in University (IRT1117), the Program of Shanghai Subject Chief Scientist (12XD1405900), and the Shanghai Leading Academic Discipline Project (B108).

Notes and references

1 Special issue, N. Tinanoff, *Int. J. Clin. Dent.*, 1995, **6**, 37.
2 H. J. Keene, I. L. Shklair and G. J. Mickel, *J. Dent. Res.*, 1977, **56**, 21.
3 (*a*) H. Rudel, *Ecotoxicol. Environ. Saf.*, 2003, **56**, 180; (*b*) S. G. Schäfer and U. Femfert, *Regul. Toxicol. Pharmacol.*, 1984, **4**, 57.
4 N. Cardarelli, *Thymus*, 1990, **15**, 223.
5 L. R. Sherman, J. Masters, R. Peterson and S. Levine, *J. Anal. Toxicol.*, 1986, **10**, 6.
6 S. Ulusoy, H. I. Ulusoy and M. Akcay, *Food Chem.*, 2012, **134**, 419.
7 M. Arvand, A. M. Moghimi, A. Afshari and N. Mahmoodi, *Anal. Chim. Acta*, 2006, **579**, 102.
8 (*a*) X. R. Huang, W. J. Zhang, S. H. Han and X. Q. Wang, *Talanta*, 1997, **44**, 817; (*b*) T. Madrakian and F. Ghazizadeh, *J. Braz. Chem. Soc.*, 2009, **20**, 1535.
9 Q. Wang, C. Li, Y. Zou, H. Wang, T. Yi and C. Huang, *Org. Biomol. Chem.*, 2012, **10**, 6740.
10 J. Liu, K. Wu, X. Li, Y. F. Han and M. Xia, *RSC Adv.*, 2013, **3**, 8924.
11 (*a*) S. K. Ko, Y. K. Yang, J. Tae and I. Shin, *J. Am. Chem. Soc.*, 2006, **128**, 14150; (*b*) J. Y. Kwon, Y. J. Jang, Y. J. Lee, K. M. Kim, M. S. Seo, W. Nam and J. Yoon, *J. Am. Chem. Soc.*, 2005, **127**, 10107.
12 S. Kenmoku, Y. Urano, H. Kojima and T. Nagano, *J. Am. Chem. Soc.*, 2007, **129**, 7313.
13 J. M. Sanfrutos, J. L. Jaramillo, M. O. Munoz, M. A. Fernandez, F. P. Balderas, F. H. Mateo and F. S. Gonzalez, *Org. Biomol. Chem.*, 2010, **8**, 667.
14 Y. Shiraishi, R. Miyamoto, X. Zhang and T. Hirai, *Org. Lett.*, 2007, **9**, 3921.
15 H. Yang, Z. Zhou, K. Huang, M. Yu, F. Li, T. Yi and C. Huang, *Org. Lett.*, 2007, **9**, 4729.
16 R. E. Melendez and W. D. Lubell, *J. Am. Chem. Soc.*, 2004, **126**, 6759.
17 C. Y. Li, Y. Liu, Y. Q. Wu, Y. Sun and F. Y. Li, *Biomaterials*, 2013, **34**, 1223.
18 A. K. Mahapatra, S. K. Manna and D. Mandal, *Inorg. Chem.*, 2013, **52**, 10825.
19 R. L. Sheng, P. F. Wang, Y. H. Gao, Y. Wu, W. M. Liu, J. J. Ma, H. P. Li and S. K. Wu, *Tetrahedron*, 2010, **66**, 9655.
20 A. K. Mahapatra, S. K. Manna, D. Mandal and C. D. Mukhopadhyay, *J. Med. Chem.*, 1993, **36**, 1839.
21 (*a*) H. L. Li, J. L. Fan, F. L. Song, H. Zhu, J. J. Du, S. G. Sun and X. J. Peng, *Chem.–Eur. J.*, 2010, **16**, 12349; (*b*) J. F. Zhang, Y. Zhou, J. Yoon, Y. Kim, S. J. Kim and J. S. Kim, *Org. Lett.*, 2010, **12**, 3852; (*c*) Z. X. Han, X. B. Zhang, L. Zhuo, Y. J. Gong, X. Y. Wu, J. Zhen, C. M. He, L. X. Jian, Z. Jing, G. L. Shen and R. Q. Yu, *Anal. Chem.*, 2010, **82**, 3108.
22 (*a*) Z. Li, Y. L. Song, Y. H. Yang, L. Yang, X. H. Huang, J. H. Han and S. F. Han, *Chem. Sci.*, 2012, **3**, 2941; (*b*) S. Q. Wu, Z. Li, J. H. Han and S. F. Han, *Chem. Commun.*, 2011, **47**, 11276; (*c*) I. Meerovich, A. Koshkaryev, R. Thekkedath and V. P. Torchilin, *Bioconjugate Chem.*, 2011, **22**, 2271.
23 L. Xue, G. P. Li, D. J. Zhu, Q. Liu and H. Jiang, *Inorg. Chem.*, 2012, **51**, 10842.